J. Fluid Mech. (2000), *vol.* 404, *pp.* 27–46. Printed in the United Kingdom

Control action for stabilizing free shear layers

By J. E. FFOWCS WILLIAMS[1] AND W. MÖHRING[2]

[1] Department of Engineering, University of Cambridge, Trumpington Street, Cambridge CB2 1PZ, UK

[2] Max-Planck-Institut für Strömungsforschung, Göttingen, Germany

(Received 22 October 1998 and in revised form 7 October 1999)

The possibility of acoustic control of the two-dimensional instabilities of a lossless plane shear layer of vanishing thickness is studied. The shear layer is formed from a body of incompressible fluid sliding over another fluid at rest. It is unstable through the generation of Kelvin–Helmholtz waves. We consider the possibility of adding to this linearly unstable flow a simple source, driven in such a way that its field interferes destructively with the instability to render the flow stable. The required strength of the unsteady control source is determined in terms of the fluctuating velocity at some fixed position in the moving fluid. We show that no unstable Kelvin–Helmholtz wave could survive the action of such a source. Next, we examine the scope for constructing the control signal from a measurement of the flow velocity at some fixed position. The source is a linear functional of the monitored velocity and we give the transfer function that would be required for the instabilities to be controlled. We prove that such control action would completely stabilize the otherwise unstable vortex sheet, and that other alternative sensor/actuator arrangements could also be effective. We go on to show that our particular very simple arrangement could not in fact be realized because, if required to work at all frequencies, it would not be causal. If we insisted on causality the vortex sheet would then only be stabilized over most frequencies. That would of course make the controlled flow completely different from the vortex sheet whose instabilities are so well known – and troublesome. We conjecture that there will exist some variations of the basic control arrangement described here that are both physically realizable and effective over the required frequency range. From our study of the initial value problem we have concluded that short perturbations would be attenuated very rapidly.

1. Introduction

Instabilities are among the most prevalent features of fluid flows. Sometimes their occurrence and their action are beneficial but much more often they show an adverse action; they transform laminar flow into turbulence. One of the greatest nuisances resulting from turbulence of high Reynolds number jets is its noise. This noise is so loud as to threaten the commercial viability of supersonic aircraft on environmental grounds. Few with knowledge of turbulence's chaotic character can hold much expectation that turbulence will ever be controlled and made quiet. Avoiding turbulence altogether might be a simpler thing to do. A steady laminar jet would be silent, but so different from a jet's natural state that should it exist at all it would only do so under highly artificial conditions. The steady, silent jet conforms with all the laws of motion but is ruled out on stability grounds. Without extraneous interference, infinitesimal

disturbances would grow and gain strength to become unmanageable and chaotic. Indeed it is this fact, that the mean flow so readily passes on its energy to parasitic eddies, that accounts for the robustness of shear layer turbulence.

Is it conceivable that the normal instability of the shear layer, the root cause of the jet's turbulence and noise, might possibly be avoided by active control? The benefits of control would surely be enormous and could well be sought if only one knew how to approach the problem. Control is bound to be difficult and may well turn out to be impractical but, from the results of the model considered below, we see no grounds for thinking the concept impossible. A review of the current approaches with an emphasis on the mathematical techniques is presented in Moin & Bewley (1994). An excellent presentation of the control theory for systems having a finite number of degrees of freedom is given by Callier & Desoer (1991). Experiments to influence the growth rates of shear layer perturbations have also been performed, see e.g. Ronneberger & Ackermann (1979), Arbey & Ffowcs Williams (1984) and the recent survey by Fiedler (1998).

Here we perform a thorough study of the control of one of the simplest hydrodynamic instabilities by a very simple control system. We consider the two-dimensional Kelvin–Helmholtz instability of a shear layer, which is formed if some body of fluid moves with constant velocity above another part at rest. This system has infinite extent and an infinite number of degrees of freedom. We assume throughout that the perturbations of the shear layer are small, such that linearization is legitimate.

It is well known that unstable modes of the thin shear layer consist of plane waves moving with half the speed of the moving fluid in the direction of the moving fluid. All these Kelvin–Helmholtz waves are unstable with an amplification rate equal to the angular frequency. Conversely, to every positive angular frequency and amplification rate, which is equal to the angular frequency, there corresponds an unstable Kelvin–Helmholtz wave. We introduce into this system an unsteady point source. This problem with a prescribed source strength has been studied before by Jones & Morgan (1972), Bechert & Michel (1975) and Ffowcs Williams (1982). However, we make the source strength proportional to the velocity at some other position in the flow. The eigenfunctions of this modified system are no longer the Kelvin–Helmholtz waves but are given by a superposition of a Kelvin–Helmholtz wave and the point source with a definite relation between the amplitudes of both. The point source solution has been derived by the above mentioned authors with other applications in mind. Their solutions are not really simple and tailoring one of them to our application is not completely trivial. We therefore rederive the point source solution by a different method and show that the Ffowcs Williams solution can be obtained from our solution. This approach has furthermore the advantage of making the presentation self-contained. Notice that we have ignored any interaction of the source with the trailing edge which occurs at the beginning of the shear layer, see e.g. Bechert & Michel (1975) and Crighton (1985). Modifications are therefore required if the control system is close to the trailing edge.

One might expect that little can be done with the addition of a finite system to a flow of infinite extent and think that the the angular frequencies and growth rates of the instability modes cannot be influenced by this local change of the system. This, as we will see, turns out to be correct. One can determine for every frequency an impedance such that there is at that frequency a solution which remains bounded, but otherwise the mode spectrum remains unchanged. This changes drastically if one admits impedances which depend on the frequency. Then one can determine an impedance such that there are bounded solutions for all frequencies. This impedance,

our goal impedance, is chosen in such a manner that the Kelvin–Helmholtz wave which is generated by the source cancels the incident Kelvin–Helmholtz wave. The source strength and the amplitude of an incident Kelvin–Helmholtz wave are then closely interrelated. We will consider only this choice of the impedance, then each stability mode can be characterized either by the strength of the incident Kelvin–Helmholtz wave or by the strength of the source. Here it is important to realize that there is only one unstable Kelvin–Helmholtz wave to every frequency. Therefore one might expect that a proper choice of the impedance for each frequency is sufficient to control the Kelvin–Helmholtz waves for all frequencies.

We are interested in real frequencies, which are often studied in hydrodynamic stability problems with the idea of spatial amplification in mind. It is perhaps not surprising that the solutions remain bounded in the whole space for real frequencies for our goal impedance also. The controlled shear layer is stable under spatial amplification.

This goal impedance is not an analytic function of the frequency ω in the upper complex ω-half-plane. This implies, see e.g. Landau & Lifschitz (1966), that the source strength depends not only on the previous sensor values, but also on future values. Our goal impedance is not causal. It turns out that this non-causality originates from the non-causal character of the Kelvin–Helmholtz wave as it is not an analytic function in the upper ω-half-plane. The source solution is causal. If one thinks of a Kelvin–Helmholtz wave as being generated by some source it would of course be a causal function. The non-causality enters when one performs the limiting process that leads to the pure Kelvin–Helmholtz mode, the limit as the source position approaches $-\infty$. This difference which should be of little physical significance simplifies the mathematics significantly. We will therefore study the system with our goal impedance. We obtain the very interesting result that the imaginary part of the impedance is positive for positive frequencies, provided the sensor position is not too far upstream or too far downstream of the source position. In Landau & Lifschitz (1966) it is shown that this leads to a positive generalized 'dissipation' and would exclude unstable modes, if the impedance were causal. For a real system the impedance has to be causal. So we have to approximate our goal system by a causal one. The question of a good or even of the best causal approximation is a difficult one and outside the range of this investigation. We show however that a small deviation from the goal impedance at some value of the frequency leads to a significant reduction of the amplitude of an incoming wave at that frequency. It is therefore not absolutely necessary to generate the goal impedance exactly. As a causal impedance has to differ from any non-causal one over some range of frequencies, a large reduction cannot be achieved for all frequencies, and so a causal impedance can work only for most frequencies. One also wants the real system to be stable. To achieve this, a sensor position with positive generalized dissipation is sensible. This requires that the sensor is placed not too far away from the source position. Notice that our equation for the impedance shows that complete cancellation can be obtained for every sensor position. The governing equations are elliptic; there are no well-defined influence regions. An attempt to couple the source to a far away sensor leads to instabilities however.

We have designed the impedance such that a control of incident Kelvin–Helmholtz waves is achieved. To study the effect of this control scheme on other perturbations, we determined the solutions generated by point sources. As the point source solution far downstream is dominated by Kelvin–Helmholtz waves one expects that the scheme should be effective if the point source is located upstream of the sensor position. This is exactly what we find. The amplitude of the Kelvin–Helmholtz wave radiated from

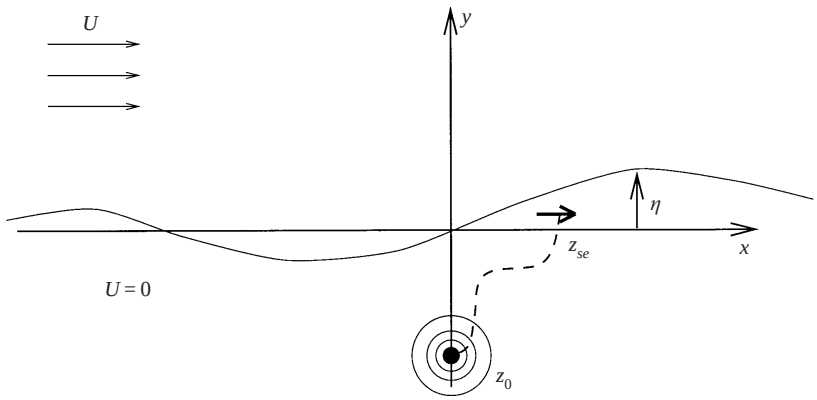

FIGURE 1. Sketch of the flow region with the shear layer and the control loop between the velocity sensor and the loudspeaker.

the point source is significantly reduced if the point source is situated in a certain 90°-sector upstream of the sensor position. The frequency dependence of this sector is small.

We also determine the response of the shear layer which is controlled with our goal impedance to a short time disturbance and compare it to the response of the uncontrolled shear layer. We assume that the disturbance requires a perturbation of the control loudspeaker in the form of a Dirac δ-function in time and find a significant motion of the shear layer only near the excitation time. It grows exponentially before the δ-function control pulse and decays exponentially thereafter. There is no indication of an instability. This is in marked contrast to an uncontrolled shear layer, where a finite time singularity occurs.

2. Basic relations

We consider small perturbations of an infinite incompressible shear layer (figure 1). We assume that the unperturbed shear layer is at $y = 0$ and that there is a flow of uniform velocity U for $y > 0$ and no velocity for $y < 0$. Let $y = \eta(x, t)$ be the position of the perturbed shear layer. We require it to be small, such that higher-order contributions may be neglected and that the boundary conditions can be fulfilled at $y = 0$. The flow in both half-planes $y < 0$ and $y > 0$ can be described by potentials φ_n, by stream functions ψ_n or by complex potentials $F_n = \varphi_n + \mathrm{i}\psi_n$. The index 1 refers to the upper half-plane with flow and the index 2 to the lower half-plane.

To fulfil the boundary conditions at the shear layer, we reflect the flow in the lower half-plane into the upper half-plane by replacing

$$y \to -y,\ v_2 \to -v_2,\ \psi_2 \to -\psi_2, \quad \text{i.e. } \tilde{F}_2 = \overline{F_2(\bar{z})},$$

where the overbar denotes the conjugate complex. Then the reflected complex potential of the flow in the lower half-plane $\tilde{F}_2$ is again an analytic function of $z = x + \mathrm{i}y$ which is however now defined in the upper half-plane. In the following we will for simplicity omit the tilde, as the original F_2 defined in the lower half-plane is never used again. The reason for this transformation will become clear later. At the vortex sheet one has the equality of pressure which can be written from the Bernoulli equation in

terms of the complex potential as

$$\mathrm{Re}\left(\frac{\mathrm{D}F_1}{\mathrm{D}t}-\frac{\partial F_2}{\partial t}\right)=0 \quad \text{with } \frac{\mathrm{D}}{\mathrm{D}t}=\frac{\partial}{\partial t}+U\frac{\partial}{\partial z} \tag{2.1}$$

at the vortex sheet. The continuity of particle displacement at the vortex sheet $y=\eta(x,t)$ leads to

$$\frac{\partial\eta}{\partial t}+U\frac{\partial\eta}{\partial x}=-\frac{\partial\psi_1}{\partial x}, \quad \frac{\partial\eta}{\partial t}=-\frac{\partial\psi_2}{\partial x}$$

and therefore

$$\frac{\partial^2\psi_2}{\partial x\partial t}+U\frac{\partial^2\psi_2}{\partial x^2}=-\frac{\partial^2\psi_1}{\partial x\partial t}$$

at the vortex sheet. Omitting an arbitrary integration constant which may depend on y and t, one can write

$$\mathrm{Im}\left(\frac{\mathrm{D}F_2}{\mathrm{D}t}+\frac{\partial F_1}{\partial t}\right)=0 \tag{2.2}$$

at the vortex sheet. We now write

$$\frac{\mathrm{D}F_1}{\mathrm{D}t}-\frac{\partial F_2}{\partial t}=f(z,t) \quad \text{and} \quad \frac{\mathrm{D}F_2}{\mathrm{D}t}+\frac{\partial F_1}{\partial t}=g(z,t) \tag{2.3}$$

and observe that f and g are analytic functions of z in the upper half-plane, provided there are no obstacles in the upper and lower half-planes. Here the reason for the reflection into the upper half-plane becomes clear. Only the reflected F_2 is analytic in the upper half-plane. The original unreflected F_2 is analytic in the lower half-plane. Furthermore we conclude from (2.1) that $f(z,t)$ has vanishing real part at $y=0$ and from (2.2) that $g(z,t)$ has a vanishing imaginary part there. By these properties one is often able to determine the functions f and g by function theoretic arguments. For a stability analysis of these equations, one would like to introduce a second imaginary unit j and assume that all quantities are proportional to $\exp(-\mathrm{j}\omega t)$. This can be done if sufficient care is taken, see e.g. Möhring (1975). An alternative approach has been used in Bechert & Michel (1975). Then all quantities Z are with real Z_r, Z_i, Z_j, Z_{ij} of the form

$$Z=Z_r+\mathrm{i}Z_i+\mathrm{j}Z_j+\mathrm{ij}Z_{ij}.$$

One has the relations

$$(1\mp\mathrm{ij})\mathrm{j}=\pm(1\mp\mathrm{ij})\mathrm{i} \quad \text{and} \quad (1-\mathrm{ij})(1+\mathrm{ij})=0 \tag{2.4}$$

and for every Z

$$Z=\frac{1-\mathrm{ij}}{2}\hat{Z}+\frac{1+\mathrm{ij}}{2}\check{Z}=\frac{1-\mathrm{ij}}{2}\acute{Z}+\frac{1+\mathrm{ij}}{2}\grave{Z}, \tag{2.5}$$

where $\hat{Z}$ and $\check{Z}$ are obtained from Z if every j in Z is replaced by i and $-\mathrm{i}$ respectively. Similarly $\acute{Z}$ and $\grave{Z}$ are obtained from Z if every i in Z is replaced by j and $-\mathrm{j}$ respectively. The numbers containing i and j can by multiplication with $1-\mathrm{ij}$ or $1+\mathrm{ij}$ be reduced to ordinary complex numbers with imaginary units i or j. This is the reason for the frequent occurrence of the factors $1\pm\mathrm{ij}$ in later equations. Equation (2.4) shows that the product of non-zero factors can be zero; division can therefore be performed only if sufficient care is taken. Equation (2.3) can then be written as

$$U\frac{\mathrm{d}F_1}{\mathrm{d}z}=\mathrm{j}\omega F_1-\mathrm{j}\omega F_2+f(z), \qquad U\frac{\mathrm{d}F_2}{\mathrm{d}z}=\mathrm{j}\omega F_1+\mathrm{j}\omega F_2+g(z)$$

or in matrix notation

$$\frac{\mathrm{d}\boldsymbol{F}}{\mathrm{d}z} = \boldsymbol{B}\boldsymbol{F} + \boldsymbol{f} \tag{2.6}$$

with

$$\boldsymbol{F} = \begin{pmatrix} F_1 \\ F_2 \end{pmatrix}, \quad \boldsymbol{B} = \frac{\mathrm{j}\omega}{U}\begin{pmatrix} 1 & -1 \\ 1 & 1 \end{pmatrix}, \quad \boldsymbol{f} = \frac{1}{U}\begin{pmatrix} f \\ g \end{pmatrix}.$$

As (2.3) are real with respect to j, one has for the F_n the reality relations

$$F_n(\omega) = F_n^*(-\omega^*), \tag{2.7}$$

where F_n^* denotes the complex conjugate of F_n with respect to j, i.e. every j occurring in Z is to be replaced by $-\mathrm{j}$. Equation (2.7) shows that the values of F_n for ω having a negative real part can easily be determined from those of the positive real part. It states that taking the real part amounts to the same as summing over positive and negative frequencies. Equation (2.6) can be solved by the method of variation of parameters. One needs a fundamental system of the homogeneous equation (2.6). It is not difficult to show that one has

$$\frac{\mathrm{d}\boldsymbol{\Phi}(z)}{\mathrm{d}z} = \boldsymbol{B}\boldsymbol{\Phi}(z) \quad \text{for } \boldsymbol{\Phi}(z) = \begin{pmatrix} \mathrm{e}^{\gamma_1 z} & -\mathrm{e}^{\gamma_2 z} \\ \mathrm{j}\mathrm{e}^{\gamma_1 z} & \mathrm{j}\mathrm{e}^{\gamma_2 z} \end{pmatrix} \tag{2.8}$$

with

$$\gamma_{1,2} = \frac{\omega}{U}(\pm 1 + \mathrm{j}). \tag{2.9}$$

If one now assumes $\boldsymbol{F} = \boldsymbol{\Phi}\boldsymbol{b}$ one obtains from (2.6)

$$\frac{\mathrm{d}\boldsymbol{b}}{\mathrm{d}z} = \boldsymbol{\Phi}^{-1}\boldsymbol{f} \quad \text{with } \boldsymbol{\Phi}^{-1} = \frac{1}{2}\begin{pmatrix} \mathrm{e}^{-\gamma_1 z} & -\mathrm{j}\mathrm{e}^{-\gamma_1 z} \\ -\mathrm{e}^{-\gamma_2 z} & -\mathrm{j}\mathrm{e}^{-\gamma_2 z} \end{pmatrix}$$

and therefore

$$\boldsymbol{b} = \begin{pmatrix} b_1 \\ b_2 \end{pmatrix} = \frac{1}{2U}\begin{pmatrix} \displaystyle\int_0^z \mathrm{e}^{-\gamma_1\zeta}(f(\zeta) - \mathrm{j}g(\zeta))\,\mathrm{d}\zeta + c_1 \\ \displaystyle -\int_0^z \mathrm{e}^{-\gamma_2\zeta}(f(\zeta) + \mathrm{j}g(\zeta))\,\mathrm{d}\zeta + c_2 \end{pmatrix} \tag{2.10}$$

and

$$\boldsymbol{F} = \boldsymbol{\Phi}_0\begin{pmatrix} \mathrm{e}^{\gamma_1 z} b_1(z) \\ \mathrm{e}^{\gamma_2 z} b_2(z) \end{pmatrix} \quad \text{with } \boldsymbol{\Phi}_0 = \boldsymbol{\Phi}|_{z=0} = \begin{pmatrix} 1 & -1 \\ \mathrm{j} & \mathrm{j} \end{pmatrix}. \tag{2.11}$$

3. Stability of shear layers

3.1. *Time-harmonic perturbations*

We describe first the well-known stability modes of the infinite shear layer. There the complex potentials F_1 and F_2 are regular in the upper half-plane and decay at infinity. Equation (2.3) shows that this is also true for f and g. Furthermore f is purely imaginary at the shear layer, i.e. at the real axis and g purely real there. Then both possess by the Schwarz reflection principle an analytic continuation into the whole complex plane and therefore vanish by Liouville's theorem. The complex potentials are therefore given by a solution of the homogeneous equation (2.8), i.e.

$$F = \mathrm{e}^{\gamma_{1,2} z - \mathrm{j}\omega t} = \exp\left(\mathrm{j}\omega\left(\frac{z}{U} - t\right) \pm \frac{\omega z}{U}\right) \tag{3.1}$$

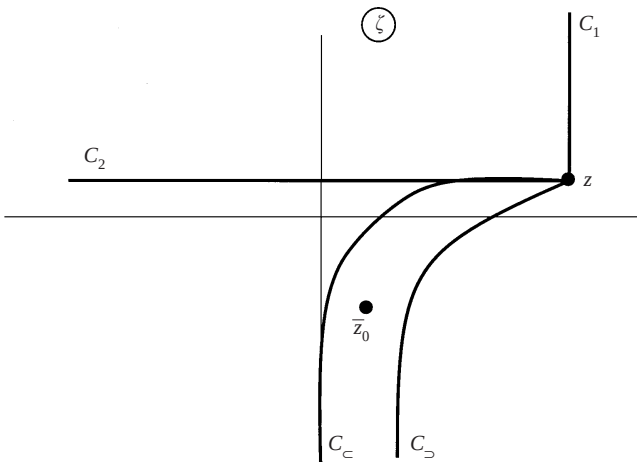

FIGURE 2. The integration paths used in the determination of the complex potentials.

with $\gamma_{1,2}$ from (2.9). The potentials describing spatial amplification are directly obtained from (2.9) and (3.1) with real ω

$$F = (1 - \mathrm{ij}) \exp\left(\mathrm{j}\omega\left(\frac{z}{U} - t\right) \pm \frac{\omega z}{U}\right). \tag{3.2}$$

An attempt to control the shear layer can be made by introducing a source in the no-flow region and coupling its amplitude to some flow quantity. So let us first solve the problem of a source near a shear layer. Let

$$\Delta(z) = Q \log(z - z_0) \quad \text{and} \quad \overline{\Delta(\overline{z})} = Q \log(z - \overline{z_0}) \quad \text{with } \mathrm{Im_i}\, Q = 0 \tag{3.3}$$

denote the complex potential of a source of strength Q at z_0 and of its mirror reflection at the real axis. The overbar denotes the complex conjugate with respect to i, i.e. every i is replaced by $-$i. We assume that the source is situated in the no-flow region in the lower half-plane and that it has the usual time dependence proportional to $\exp(-\mathrm{j}\omega t)$, i.e. $\partial/\partial t \to -\mathrm{j}\omega$. Δ of (3.3) denotes its reflection into the upper half-plane, i.e. $\mathrm{Im_i}\, z_0 > 0$. Then the functions f and g are no longer analytic in the upper half-plane but both have a pole at $z = z_0$. They can be determined from (2.3) as

$$f = \mathrm{j}\omega(\Delta(z) - \overline{\Delta(\overline{z})}), \qquad g = \frac{\mathrm{D}\Delta(z)}{\mathrm{D}t} + \frac{\mathrm{D}\overline{\Delta(\overline{z})}}{\mathrm{D}t}. \tag{3.4}$$

This addition of the mirror images makes f purely imaginary and g purely real (with respect to i) on the real axis. Then one can rewrite (2.3) as

$$\frac{\mathrm{D}F_1 - \overline{\Delta(\overline{z})}}{\mathrm{D}t} - \frac{\partial F_2 - \Delta(z)}{\partial t} = -U\frac{\mathrm{d}\overline{\Delta(\overline{z})}}{\mathrm{d}z} \quad \text{and} \quad \frac{\mathrm{D}F_2 - \Delta(z)}{\mathrm{D}t} + \frac{\partial F_1 - \overline{\Delta(\overline{z})}}{\partial t} = U\frac{\mathrm{d}\,\overline{\Delta(\overline{z})}}{\mathrm{d}z} \tag{3.5}$$

with right-hand sides which are analytic in the upper half-plane. One can use the

general solution of (2.11) and write for $\boldsymbol{F}$

$$\boldsymbol{F} = \begin{pmatrix} \overline{\Delta(\overline{z})} \\ \Delta(z) \end{pmatrix} + \boldsymbol{\Phi}_0 \begin{pmatrix} -\dfrac{1+\mathrm{j}}{2} Q \exp\left(\dfrac{(1+\mathrm{j})\omega}{U} z\right) \oint_{-\mathrm{j}\infty}^{z} \dfrac{\exp(-[(1+\mathrm{j})\omega/U]\zeta)}{\zeta - \overline{z_0}} \,\mathrm{d}\zeta \\ \dfrac{1-\mathrm{j}}{2} Q \exp(-[(1-\mathrm{j})\omega/U]z) \displaystyle\int_{-\infty}^{z} \dfrac{\exp([(1-\mathrm{j})\omega/U]\zeta)}{\zeta - \overline{z_0}} \,\mathrm{d}\zeta \end{pmatrix}. \tag{3.6}$$

Additionally Kelvin–Helmholtz (3.1) waves could be added. We have specified the lower integration limits in the integrals in (3.6) such as to obtain a source solution which decays in the far field – aside from the logarithmic terms in $\Delta(z)$ and $\overline{\Delta(\overline{z})}$. $\oint$ denotes that the integration path stays to the left of the pole at $\zeta = \overline{z_0}$ ($C_{\subset}$ in figure 2). We will see that this leads to a solution fulfilling a radiation condition. We require that the integration path in the lower integral in (3.6) remains everywhere in the upper half-plane (e.g. along C_2 in figure 2). The upper integral contains the second imaginary unit j in the integrand and the integration boundary. This is a shorthand notation for

$$\oint_{-\mathrm{j}\infty}^{z} \frac{\exp(-[(1+\mathrm{j})\omega/U]\zeta)}{\zeta - \overline{z_0}} \,\mathrm{d}\zeta = \frac{1-\mathrm{ij}}{2} \oint_{-\mathrm{i}\infty}^{z} \frac{\exp(-[(1+\mathrm{i})\omega/U]\zeta)}{\zeta - \overline{z_0}} \,\mathrm{d}\zeta + \frac{1+\mathrm{ij}}{2} \int_{\mathrm{i}\infty}^{z} \frac{\exp([(1-\mathrm{i})\omega/U]\zeta)}{\zeta - \overline{z_0}} \,\mathrm{d}\zeta.$$

Both integrals are exponential integrals, see Abramowitz & Stegun (1965), with their singularity at $\zeta = \overline{z_0}$. Because of that pole, the values of the integrals depend on the integration path. The second integral is well defined, if we restrict the integration path to the upper half-plane (e.g. along C_1 in figure 2). In the first integral, the integration path passes to the left of $\zeta = \overline{z_0}$ and one obtains

$$\begin{aligned} I_1 &= \exp\left(\frac{(1+\mathrm{j})\omega z}{U}\right) \oint_{-\mathrm{j}\infty}^{z} \frac{\exp(-(1+\mathrm{j})\omega\zeta/U)}{\zeta - \overline{z_0}} \,\mathrm{d}\zeta \\ &= \exp\left(\frac{(1+\mathrm{j})\omega(z-\overline{z_0})}{U}\right) E\left(-\frac{(1+\mathrm{j})\omega(z-\overline{z_0})}{U}\right), \end{aligned} \tag{3.7}$$

where E denotes the exponential integral

$$E(z) = \int_{-\infty}^{z} \frac{\mathrm{e}^{\zeta}}{\zeta} \,\mathrm{d}\zeta. \tag{3.8}$$

The exponential integral is a multivalued function and it is important to use the values from the correct branch in (3.7). We are interested in z-values in the upper i-half-plane and in ω-values in the upper j-half-plane. With the representation (2.5) the integral (3.7) can be written as a sum of two contributions, both of which contain only, apart from the $1 \pm \mathrm{ij}$-factors, the imaginary unit j. Then the two complex half-planes together form a complete complex plane and it is necessary to determine the correct location of the branch cut and the correct branch. To be specific, we denote by $E^{\alpha}(z)$ that branch of the exponential integral which vanishes at $z \to -\infty$ and has its branch cut at $\arg z = \alpha$ with α between $-\pi$ and π. $E^{\alpha}(z)$ is then real for negative

real z. We use (2.5) to express (3.7) in the plane with the imaginary unit j and write

$$I_1 = \frac{1-\mathrm{ij}}{2}\exp\left(\frac{(1+\mathrm{j})\omega(\acute{z}-\acute{\overline{z_0}})}{U}\right)E^{-3\pi/4}\left(-\frac{(1+\mathrm{j})\omega(\acute{z}-\acute{\overline{z_0}})}{U}\right)$$
$$+\frac{1+\mathrm{ij}}{2}\exp\left(\frac{(1+\mathrm{j})\omega(\grave{z}-\grave{\overline{z_0}})}{U}\right)E^{\pi/4}\left(-\frac{(1+\mathrm{j})\omega(\grave{z}-\grave{\overline{z_0}})}{U}\right)$$
$$=\frac{1-\mathrm{ij}}{2}E\mathrm{e}^{-3\pi/4}\left(-\frac{(1+\mathrm{j})\omega(\acute{z}-\acute{\overline{z_0}})}{U}\right)+\frac{1+\mathrm{ij}}{2}E\mathrm{e}^{\pi/4}\left(-\frac{(1+\mathrm{j})\omega(\grave{z}-\grave{\overline{z_0}})}{U}\right), \tag{3.9}$$

where we have written

$$E\mathrm{e}^{\alpha} = \mathrm{e}^{-z}\,E^{\alpha}(z)$$

as shorthand. We have already indicated the correct branches. Let us explain briefly the determination of the branch cut in the first integral. The phase angle of ω varies between 0 and π in the complex j-plane. The same is true of $\acute{z}-\acute{\overline{z_0}}$. Then the phase angle of $\omega(\acute{z}-\acute{\overline{z_0}})$ varies between 0 and 2π and that of the argument of the first exponential integral between $-\frac{3}{4}\pi$ and $\frac{5}{4}\pi$. Integrating on the negative real axis keeps the integration path to the left of the pole at $\zeta = \overline{z_0}$. Similar arguments determine the second contribution in (3.9), the main difference being that the phase angle $\grave{z}-\grave{\overline{z_0}}$ varies between $-\pi$ and 0. One obtains for the second integral in (3.6)

$$I_2 = \exp\left(\frac{(-1+\mathrm{j})\omega z}{U}\right)\int_{-\infty}^{z}\frac{\exp\left((1-\mathrm{j})\omega\zeta/U\right)}{\zeta-\overline{z_0}}\,\mathrm{d}\zeta$$
$$=\frac{1-\mathrm{ij}}{2}\exp\left(\frac{(-1+\mathrm{j})\omega(\acute{z}-\acute{\overline{z_0}})}{U}\right)E^{-\pi/4}\left(\frac{(1-\mathrm{j})\omega(\acute{z}-\acute{\overline{z_0}})}{U}\right)$$
$$+\frac{1+\mathrm{ij}}{2}\exp\left(\frac{(-1+\mathrm{j})\omega(\grave{z}-\grave{\overline{z_0}})}{U}\right)E^{3\pi/4}\left(\frac{(1-\mathrm{j})\omega(\grave{z}-\grave{\overline{z_0}})}{U}\right)$$
$$=\frac{1-\mathrm{ij}}{2}E\mathrm{e}^{-\pi/4}\left(\frac{(1-\mathrm{j})\omega(\acute{z}-\acute{\overline{z_0}})}{U}\right)+\frac{1+\mathrm{ij}}{2}E\mathrm{e}^{3\pi/4}\left(\frac{(1-\mathrm{j})\omega(\grave{z}-\grave{\overline{z_0}})}{U}\right). \tag{3.10}$$

The potentials $\boldsymbol{F}$ are obtained as linear combination of I_1, I_2. Their asymptotic behaviour for large values of z depends on the asymptote of $E\mathrm{e}^{\alpha}(z)$ and this depends critically on α. First one observes that one always has for $\mathrm{Re}\,z > 0$

$$E\mathrm{e}^{\alpha}(z) \sim \frac{1}{z} \tag{3.11}$$

The behaviour of (3.11) is also found on the negative real axis and in the sector between the branch cut and the negative real axis. This means that (3.11) is valid everywhere if $|\alpha| < \pi/2$. If however $|\alpha| > \pi/2$ one has the sector $\pi/2 < \arg z < \alpha$ for positive α and $\alpha < \arg z < -\pi/2$ for negative α where instead of (3.11) there is exponential growth of $E\mathrm{e}^{\alpha}(z)$, namely

$$E\mathrm{e}^{\alpha}(z) \sim 2\pi\mathrm{i}\,\mathrm{sgn}\,\alpha\mathrm{e}^{-z}.$$

Equations (3.9) and (3.10) show that the I_1, I_2 and therefore also the potentials $\boldsymbol{F}$ do

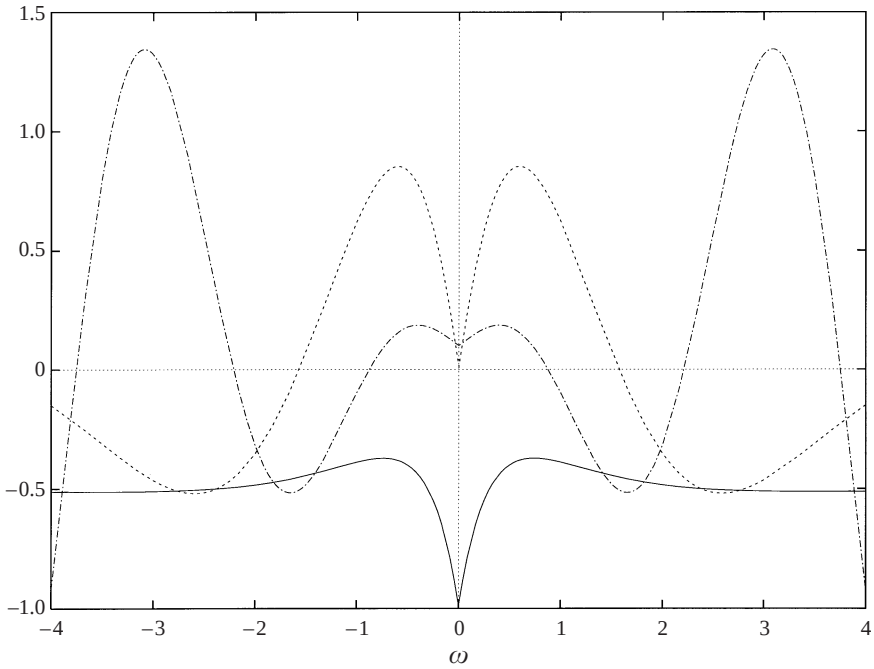

FIGURE 3. The real parts of the velocity of a free shear layer u_1 in the half-plane with flow at $y = 0$ and $x = -1$ (full), 0 (dashed), and 1.1 (dot-dashed) as function of frequency.

not decay for all z and ω in their upper complex half-planes. For positive ω, there is an exponentially growing contribution from I_1 for positive x, which is actually a Kelvin–Helmholtz wave generated by the source

$$\boldsymbol{F} = \begin{pmatrix} \overline{\Delta(\bar{z})} \\ \Delta(z) \end{pmatrix} + \boldsymbol{\Phi}_0 \begin{pmatrix} f_{KH}(z_0) Q(1 - \mathrm{ij}) \exp\left(\dfrac{(1+\mathrm{i})\omega}{U} z\right) \\ 0 \end{pmatrix}, \tag{3.12}$$

$$f_{KH} = \pi \frac{\mathrm{j} - 1}{2} \exp\left(-\frac{(1+\mathrm{i})\omega}{U} \overline{z_0}\right),$$

where contributions decaying for $|z| \to \infty$ have been neglected. Equation (3.12) shows that there is a Kelvin–Helmholtz wave of amplitude A at $x \to -\infty$ and one of an amplitude which depends on A and Q at $x \to +\infty$, i.e. the source of strength Q radiates an outgoing Kelvin–Helmholtz wave of strength $f_{KH}(z_0)Q$.

The response of the shear layer to a source of strength 1 is described by

$$\boldsymbol{F}_Q = \begin{pmatrix} \log(z - \overline{z_0}) \\ \log(z - z_0) \end{pmatrix} + \boldsymbol{\Phi}_0 \begin{pmatrix} -\dfrac{1+\mathrm{j}}{2} I_1 \\ \dfrac{1-\mathrm{j}}{2} I_2 \end{pmatrix}, \tag{3.13}$$

with I_1 and I_2 from (3.9) and (3.10). $\boldsymbol{F}_Q$ determines the values of the potentials for a harmonic varying source of strength Q. In the notation of Landau & Lifschitz (1966) it is a generalized susceptibility and should fulfil the conditions of causality and reality, i.e. it should admit an analytic continuation into the upper complex ω-half-plane and the real and imaginary parts should be even and odd functions respectively. From

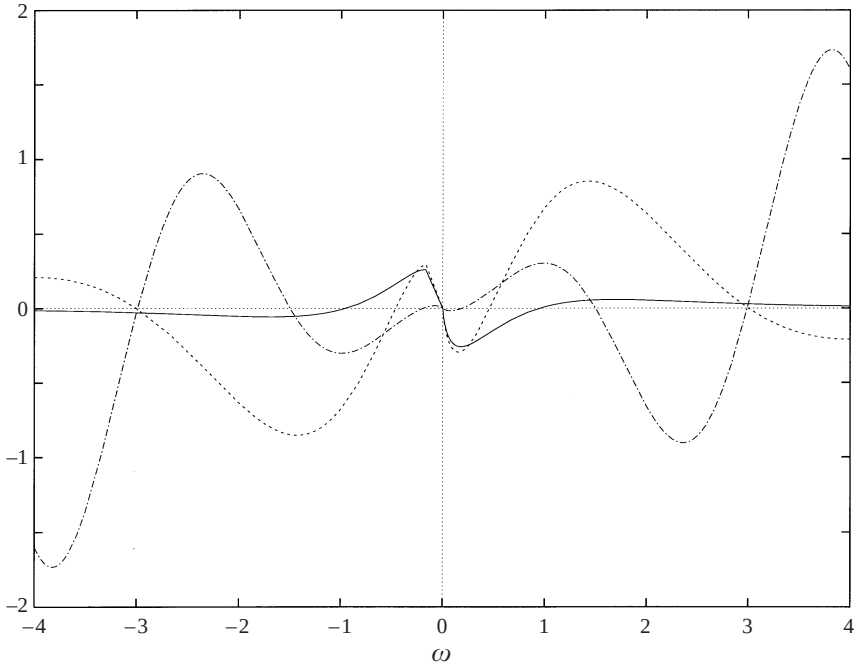

FIGURE 4. The imaginary parts of the velocity of a free shear layer u_1 in the half-plane with flow at $y = 0$ and $x = -1$ (full), 0 (dashed), and 1.1 (dot-dashed) as function of frequency.

the explicit expressions in (3.13), (3.9), (3.10), one finds that this is actually the case and that the potentials grow exponentially for large ω if $\arg(z - z_0) < \pi/4$, i.e. in the region of growth of the Kelvin–Helmholtz wave, and decay elsewhere. As an example figure 3 shows the real parts of the velocity u_1 in the half-plane with flow at $y = 0$ and $x = -1$, 0, and 1.1. The first two positions are outside the growth region of the Kelvin–Helmholtz wave, and the velocity remains bounded. The third curve (which has been multiplied by 0.1) shows the growth related to the Kelvin–Helmholtz instability. All curves are even functions of ω in agreement with the reality condition. Figure 4 shows the corresponding imaginary parts. Now the curves are odd functions of ω, again in agreement with the reality condition. Notice that the imaginary parts are negative for some positive values of the frequency. As the imaginary part determines the 'dissipation', see Landau & Lifschitz (1966), this change of sign is certainly related to the instability of the flow.

3.2. *The pulse response*

This action of the source on the shear layer can also be illustrated by a Fourier transform to derive the flow in response to a δ-function disturbance. One obtains from (3.6)

$$\boldsymbol{F} = \int_0^\infty \left[\begin{pmatrix} \overline{\Delta(\overline{z})} \\ \Delta(z) \end{pmatrix} + \boldsymbol{Q}\boldsymbol{\Phi}_0 \begin{pmatrix} -\dfrac{1+\mathrm{j}}{2} \displaystyle\oint_{(1-\mathrm{j})\infty}^{z} \dfrac{\exp\left((1+\mathrm{j})(\omega/U)(z-\zeta)\right)}{\zeta - \overline{z_0}}\,\mathrm{d}\zeta \\ \dfrac{1-\mathrm{j}}{2} \displaystyle\int_{-(1+\mathrm{j})\infty}^{z} \dfrac{\exp\left((-1+\mathrm{j})(\omega/U)(z-\zeta)\right)}{\zeta - \overline{z_0}}\,\mathrm{d}\zeta \end{pmatrix} \right] \mathrm{e}^{-\mathrm{j}\omega t}\,\mathrm{d}\omega, \tag{3.14}$$

where the incident Kelvin–Helmholtz wave has been omitted. For simplicity, we have integrated only over positive frequencies and include the contributions from negative frequencies by taking the real part. We interchange the ω- and ζ-integration and obtain for the upper integral in (3.14)

$$
\begin{aligned}
I_1 &= \int_0^\infty \oint_{(1-\mathrm{j})\infty}^{z} \frac{\exp\left(-\mathrm{j}\omega t + (1+\mathrm{j})(\omega/U)(z-\zeta)\right)}{\zeta - \overline{z_0}}\,\mathrm{d}\zeta\,\mathrm{d}\omega \\
&= \int_0^\infty \left[\frac{1-\mathrm{ij}}{2} \oint_{(1-\mathrm{i})\infty}^{z} \frac{\exp\left(-\mathrm{i}\omega t + (1+\mathrm{i})(\omega/U)(z-\zeta)\right)}{\zeta - \overline{z_0}}\,\mathrm{d}\zeta \right. \\
&\quad \left. + \frac{1+\mathrm{ij}}{2} \int_{(1+\mathrm{i})\infty}^{z} \frac{\exp\left(\mathrm{i}\omega t + (1-\mathrm{i})(\omega/U)(z-\zeta)\right)}{\zeta - \overline{z_0}}\,\mathrm{d}\zeta \right] \mathrm{d}\omega \\
&= \frac{1-\mathrm{ij}}{2} \oint_{(1-\mathrm{i})\infty}^{z} \frac{\mathrm{d}\zeta}{(\mathrm{i}t - (1+\mathrm{i})((z-\zeta)/U))(\zeta - \overline{z_0})} \\
&\quad + \frac{1+\mathrm{ij}}{2} \int_{(1+\mathrm{i})\infty}^{z} \frac{\mathrm{d}\zeta}{(-\mathrm{i}t - (1-\mathrm{i})((z-\zeta)/U))(\zeta - \overline{z_0})}
\end{aligned}
\tag{3.15}
$$

provided the integrals converge, i.e. ζ is restricted in the first integral to $\mathrm{Re}\,(1+\mathrm{i})(\zeta - z) > 0$ and to $\mathrm{Re}\,(1-\mathrm{i})(\zeta - z) > 0$ in the second. The integration paths in the integrals of (3.15) are therefore to be taken in a half-plane, which is bounded by a straight line through $\zeta = z$ of slope $\pm 45^\circ$. The integration paths are therefore not allowed to encircle the singularities originating from the first factors in the denominators of the integrands in (3.15).

We want to assume branch cuts from the poles of the integrand at $\zeta = \overline{z_0}$ and at $\zeta = z - \frac{1}{2}(1+\mathrm{j})Ut$ to $\zeta = -\infty$ and obtain

$$
\begin{aligned}
I_1 &= \frac{U}{2}(1-\mathrm{j}) \oint_{(1-\mathrm{j})\infty}^{z} \frac{\mathrm{d}\zeta}{(\zeta - z + \frac{1}{2}(1+\mathrm{j})Ut)(\zeta - \overline{z_0})} \\
&= \frac{U}{2}(1-\mathrm{j}) \frac{\log^{-\pi}(\frac{1}{2}(1+\mathrm{j})Ut) - \log^{-\pi}(z - \overline{z_0}) + (1-\mathrm{ij})\pi\mathrm{i}}{(z - \overline{z_0} - \frac{1}{2}(1+\mathrm{j})Ut)},
\end{aligned}
\tag{3.16}
$$

where $\log^{-\pi}$ denote that the branch cut has to be chosen at the negative real axis. Then the pole at $\zeta = \overline{z_0}$ is to the left of the integration path. We therefore have to subtract a residue contribution from that pole in I_1. The second integral in (3.14) is obtained from the first by replacing U by $-\mathrm{j}U$. Furthermore the integration is now extended from $\zeta = -\infty$ to z. Therefore the branch cut can be taken from the poles of the integrand to $\zeta = +\infty$ and one obtains

$$
I_2 = -U(1+\mathrm{j}) \frac{\log^{0}(\frac{1}{2}(1-\mathrm{j})2Ut) - \log^{0}(z - \overline{z_0})}{2(z - \overline{z_0} - \frac{1}{2}(1-\mathrm{j})Ut)}
$$

and therefore

$$
\boldsymbol{F} = \begin{pmatrix} \overline{\Delta(\overline{z})} \\ \Delta(z) \end{pmatrix} \delta(t) + \frac{UQ\boldsymbol{\Phi}_0}{2} \begin{pmatrix} \dfrac{\log^{-\pi}(z - \overline{z_0}) - \log^{-\pi}(\frac{1}{2}(1+\mathrm{j})Ut) - (1-\mathrm{ij})\pi\mathrm{i}}{z - \overline{z_0} - \frac{1}{2}(1+\mathrm{j})Ut} \\ \dfrac{\log^{0}(z - \overline{z_0}) - \log^{0}(\frac{1}{2}(1-\mathrm{j})Ut)}{z - \overline{z_0} - \frac{1}{2}(1-\mathrm{j})Ut} \end{pmatrix}.
$$

Now the logarithmic contributions in the first and the second component of the second column vector are just the complex conjugate with respect to j of each other if both logarithms have the branch cut at $-\pi$. Then they would contribute after multiplication with $\boldsymbol{\Phi}_0$ only to the imaginary part of $\boldsymbol{F}$, which is of no physical significance. The two branches of the logarithm differ only in the lower half-plane, namely

$$\log^0(\alpha) = \log^{-\pi}(\alpha) + 2\pi\mathrm{i}\mathrm{H}(-\mathrm{Im}\,(\alpha)),$$

where $\mathrm{H}(-\mathrm{Im}\,(\alpha))$ denotes the Heaviside-function, which is 1 for $\mathrm{Im}\,(\alpha) < 0$ and zero for $\mathrm{Im}(\alpha) > 0$. As $z - \overline{z_0}$ is restricted to the upper half-plane, one obtains contributions to $\mathrm{Re}\,\boldsymbol{F}$ only from the second logarithm

$$\mathrm{Re_j}\,\boldsymbol{F} = \begin{pmatrix} \overline{\Delta(\bar{z})} \\ \Delta(z) \end{pmatrix} \delta(t) - \frac{\pi\mathrm{i}UQ}{2}\,\mathrm{Re_j}\,\boldsymbol{\Phi}_0 \begin{pmatrix} \dfrac{1-\mathrm{ij}}{z-\overline{z_0}-\frac{1}{2}(1-\mathrm{j})Ut} \\ \dfrac{(1-\mathrm{ij})\mathrm{H}(t)+(1+\mathrm{ij})\mathrm{H}(-t)}{z-\overline{z_0}-\frac{1}{2}(1-\mathrm{j})Ut} \end{pmatrix}. \tag{3.17}$$

Now the first row is the complex conjugate of the second row for $t < 0$. A contribution to the real part is obtained only for $t > 0$, namely

$$\mathrm{Re_j}\,\boldsymbol{F} = \begin{pmatrix} \overline{\Delta(\bar{z})} \\ \Delta(z) \end{pmatrix} \delta(t) - \frac{\pi\mathrm{i}UQ}{2}\mathrm{H}(t)\,\mathrm{Re_j}\,\boldsymbol{\Phi}_0 \begin{pmatrix} \dfrac{1-\mathrm{ij}}{z-\overline{z_0}-\frac{1}{2}(1+\mathrm{i})Ut} \\ \dfrac{1-\mathrm{ij}}{z-\overline{z_0}-\frac{1}{2}(1-\mathrm{i})Ut} \end{pmatrix}. \tag{3.18}$$

The solution can be visualized as generated by two dipoles which are triggered by the source and which propagate with a velocity U and angles $\pm 45^\circ$ to the x-axis. One of them reaches the shear layer at a definite finite time and generates a singularity in the flow region. The solution vanishes for negative times; it is causal. This is exactly the solution obtained before by Ffowcs Williams (1982). Notice that the occurrence of the finite time singularity is not restricted to a δ-function-type source distribution. One obtains a source distribution with a Heaviside-function behaviour if (3.18) is integrated with respect to the time. Then a monopole singularity occurs at a finite time.

4. The controlled shear layer

Let us now assume that the motion of the shear layer consists of an incident Kelvin–Helmholtz wave and of a source and that the source strength is a linear multiple of the velocity component u in the x-direction at some sensor position z_{se} in the flow region:

$$Q = Lu(z_{se}). \tag{4.1}$$

The velocity is a superposition of a contribution from the source and from the incident Kelvin–Helmholtz wave, say

$$u(z_{se}) = Qu_Q(z_{se}) + Au_{KH}(z_{se}).$$

The control relation (4.1) then leads to

$$Q = L\left(Qu_Q(z_{se}) + Au_{KH}(z_{se})\right). \tag{4.2}$$

Because of (3.12) the amplitude of the outgoing Kelvin–Helmholtz wave is given by $f_{KH}(z_0)Q + A$. If we require it to vanish, we obtain

$$1 = L\left(u_Q(z_{se}) - f_{KH}(z_0)u_{KH}(z_{se})\right). \tag{4.3}$$

The terms in brackets depend on the frequency ω. For a constant impedance L a control of outgoing Kelvin–Helmholtz waves can be achieved but only for one value of ω. If one admits an impedance that *depends on the frequency*, one can suppress all outgoing Kelvin–Helmholtz waves if one fulfils (4.3) for all frequencies. Notice that L is *not* an analytic function of ω in the upper complex ω-half-plane. This originates not from u_Q but from u_{KH}, as we have shown in the last section that u_Q is an analytic function in the upper ω-half-plane. The Kelvin–Helmholtz wave, which we have written in (3.6) as being proportional to $\exp(\omega(1+\mathrm{j})z/U)$ should be proportional to $\exp((|\omega| + \mathrm{j}\omega)z/U)$ for all ω because of the reality condition, and this is not an analytic function of ω. This implies that the impedance L is not a causal function, i.e. the source strength determined from (4.1) depends not only on previous values of u, but also on future values. This apparently unacceptable requirement originates from the non-causality of the Kelvin–Helmholtz wave. If one observes that a source far upstream generates a Kelvin–Helmholtz wave causally, one notices that there are causal impedances which differ little from the non-causal impedance of (4.3). They depend however on the position of the upstream source and are more complicated than the impedance from (4.3). We will therefore assume (4.3) to be valid.

Here it might be useful to determine the response of the controlled shear layer to an external excitation s. So let us assume that instead of (4.1) the source strength Q is now given by

$$Q = Lu(z_{se}) + s.$$

The velocity field is again a superposition of a source and a Kelvin–Helmholtz contribution

$$u(z) = Qu_Q(z) + Au_{KH}(z) = (Lu(z_{se}) + s)u_Q(z) + Au_{KH}(z). \tag{4.4}$$

The value of u at the sensor position is now

$$u(z_{se}) = (Lu(z_{se}) + s)u_Q(z_{se}) + Au_{KH}(z_{se})$$

from which one can determine $u(z_{se})$. Inserting this value into (4.4) leads with (4.3) after some simplifications to

$$u(z) = A\left(\frac{Lu_{KH}(z_{se})}{1 - Lu_Q(z_{se})}u_Q(z) + u_{KH}(z)\right) + \frac{s}{1 - Lu_Q(z_{se})}u_Q(z) \tag{4.5}$$

$$\approx A\left(u_{KH}(z) - \frac{1}{f_{KH}(z_0)}u_Q(z)\right) + \frac{s}{Lf_{KH}(z_0)u_{KH}(z_{se})}u_Q(z), \tag{4.6}$$

where the approximate equality is true only in the working region, i.e. for those frequencies where the impedance agrees with the goal impedance. Equation (4.6) shows that an incident Kelvin–Helmholtz wave is again cancelled; the external source however generates a source solution with an associated Kelvin–Helmholtz wave. Equation (4.5) shows also that a zero of $1 - Lu_Q(z_{se})$ in the upper half-plane would lead – even for vanishing external source – to an unstable Kelvin–Helmholtz wave, i.e. the system would be unstable. The same would be true for a zero of $\tilde{L} = (1 - Lu_Q(z_{se}))/[f_{KH}(z_0)u_{KH}(z_{se})]$ as the denominator is an exponential function which does not vanish and has no singularity. Equation (4.3) shows that $\tilde{L}$ agrees in the

working region with the goal impedance. One is therefore well advised to choose a sensor position which for positive frequencies leads to a positive imaginary part of the goal impedance.

One may remark that there is not a complete suppression of the Kelvin–Helmholtz waves if (4.3) is not fulfilled exactly. A small error in (4.3) would not annihilate an incident Kelvin–Helmholtz wave completely, but would significantly reduce its amplitude. To show this let us assume that we have in (4.2) an impedance $L + \Delta L$ where L fulfils (4.3). It is easy to check that then an incident Kelvin–Helmholtz wave of amplitude A is not annihilated completely but an outgoing wave of amplitude ΔA with

$$\Delta A = \frac{u_Q(z_{se}) - f_{KH}(z_0)u_{kh}(z_{se})}{1 - (L + \Delta L)u_Q(z1)} A \Delta L$$

remains and this is small for small ΔL.

A useful result is obtained if we eliminate A in (3.6) in favour of Q. Then one observes that the Kelvin–Helmholtz term is just equal to the residue at $\zeta = \overline{z_0}$ of the integral. This means that the complex potentials of the stability modes can be written as

$$\boldsymbol{F} = \begin{pmatrix} \overline{\Delta(\bar{z})} \\ \Delta(z) \end{pmatrix} + Q\boldsymbol{\Phi}_0 \begin{pmatrix} -\dfrac{1+\mathrm{j}}{2} \not\!\!\int_{-\mathrm{j}\infty}^{z} \dfrac{\exp\left((1+\mathrm{j})(\omega/U)(z-\zeta)\right)}{\zeta - \overline{z_0}}\,\mathrm{d}\zeta \\ \dfrac{1-\mathrm{j}}{2} \displaystyle\int_{-\infty}^{z} \dfrac{\exp\left((-1+\mathrm{j})(\omega/U)(z-\zeta)\right)}{\zeta - \overline{z_0}}\,\mathrm{d}\zeta \end{pmatrix}, \tag{4.7}$$

where $\not\!\!\int$ denotes that the integration path now remains to the right of the pole at $\zeta = \overline{z_0}$ ($C_\supset$ in figure 2). It is not difficult to verify that this mode does not grow exponentially in the upper half-plane for all physically relevant frequencies with $\mathrm{Re_j}\,\omega > 0$. This is also true for purely real frequencies. This solution fulfils the control condition (4.3), and it can conveniently be used to determine the impedance L.

The integrals differ only by the residue contribution from the pole at $z = \overline{z_0}$ from the results of (3.6). We can therefore write

$$\boldsymbol{F} = \begin{pmatrix} \overline{\Delta(\bar{z})} \\ \Delta(z) \end{pmatrix} + Q\boldsymbol{\Phi}_0 \begin{pmatrix} -\dfrac{1+\mathrm{j}}{2}\left(I_1 + (1-\mathrm{ij})\pi\mathrm{j}\exp\left((1+\mathrm{j})\dfrac{\omega}{U}(\acute{z} - \acute{\overline{z_0}})\right)\right) \\ \dfrac{1-\mathrm{j}}{2} I_2 \end{pmatrix}$$

with I_1 and I_2 from (3.9) and (3.10). The solution that involves a δ-function source is again easily obtained from the solution of the free shear layer by subtraction of the residue contribution. One obtains from (3.17)

$$\mathrm{Re_j}\,\boldsymbol{F} = \begin{pmatrix} \overline{\Delta(\bar{z})} \\ \Delta(z) \end{pmatrix} \delta(t) - \frac{\pi \mathrm{i} U Q}{2} \mathrm{Re_j}\,\boldsymbol{\Phi}_0 \begin{pmatrix} 0 \\ \dfrac{(1-\mathrm{ij})\mathrm{H}(t) + (1+\mathrm{ij})\mathrm{H}(-t)}{z - \overline{z_0} - \frac{1}{2}(1-\mathrm{j})Ut} \end{pmatrix}.$$

This equation shows that the motion of a 'controlled' shear layer consistent with a δ-function perturbation of the control source begins at $t = -\infty$, well before the onset of the control perturbation, and extends to $t = \infty$. The incident instability mode of course is not caused by the controller; it consists of a dipole moving in the mirror image plane and approaching the physical half-plane which has a strength opposite to that which occurs in the free shear layer solution of Ffowcs Williams. At $t = 0$ it reaches the image of the source and cancels the dipole which eventually leads to

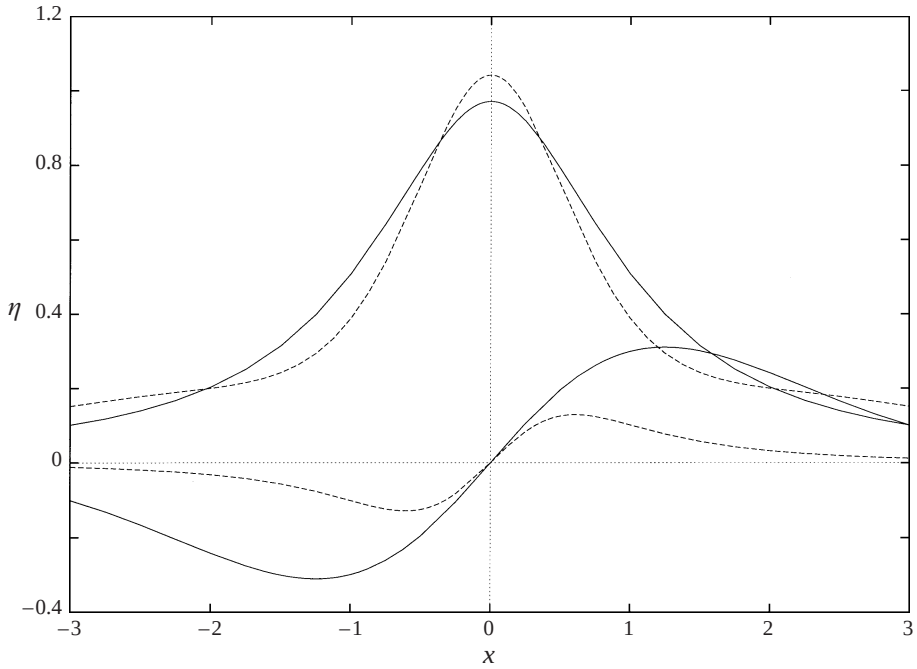

FIGURE 5. The real and imaginary parts of the shear layer displacement of the controlled shear layer for frequencies $\omega = 1$ (full) and $\omega = 5$ (dashed) as function of x. The real parts are approximately even, the imaginary parts odd, functions of x. The point source is situated at $z_0 = 0 - \mathrm{i}$. The velocity U is assumed as $U = 1$.

the singularity in the physical space. For positive times only the dipole moving in the direction away from the shear layer remains.

Some numerical results concerning the controlled shear layer are shown in figures 5 to 7. We restrict ourselves to positive frequencies and assume a continuation to negative frequencies with the reality condition. The non-causal character of these solutions is not considered to be serious. In figure 5 the real and imaginary parts $y = \eta(x)$ of the particle displacements of the controlled shear layer in arbitrary units are shown for frequencies $\omega = 1$ and $\omega = 5$. The source is in the lower no-flow half-plane with $z_0 = x_0 + \mathrm{i}y_0 = \mathrm{i}$ if reflected into the upper half-plane; the velocity U is chosen as $U = 1$. It is of course independent of the sensor position, as the necessary source strength required is determined by the incident Kelvin–Helmholtz wave. The displacements are approximately symmetric around $x = 0$; an exponential growth does not occur. There is little dependence on ω of the real part (which is approximately an even function) and a noticeable dependence on ω of the imaginary part. The real parts of the impedance determined from (4.3) are shown in figure 6. Three different sensor positions are shown, namely $z_{se} = x_{se} + \mathrm{i}y_{se} = \pm 0.3$ and $z_{se} = 0.6$. The real parts at $z_{se} = \pm 0.3$ differ only in sign.This is understandable if one compares it with the shear layer displacements from figure 5. In figure 7 the imaginary parts are shown at $z_{se} = 0.3$ and at $z_{se} = 0.6$. They would be identical at $z_{se} = -0.3$ and at $z_{se} = -0.6$. It seems very remarkable that the imaginary part is positive for positive frequencies at $z_{se} = 0.3$ and has both signs for the larger z_{se}. This implies a positive 'dissipation' for all frequencies for $z_{se} = 0.3$. This is in marked contrast to the behaviour of the uncontrolled shear layer shown in figure 4. In figure 8 the non-causal impedance is compared with a causal

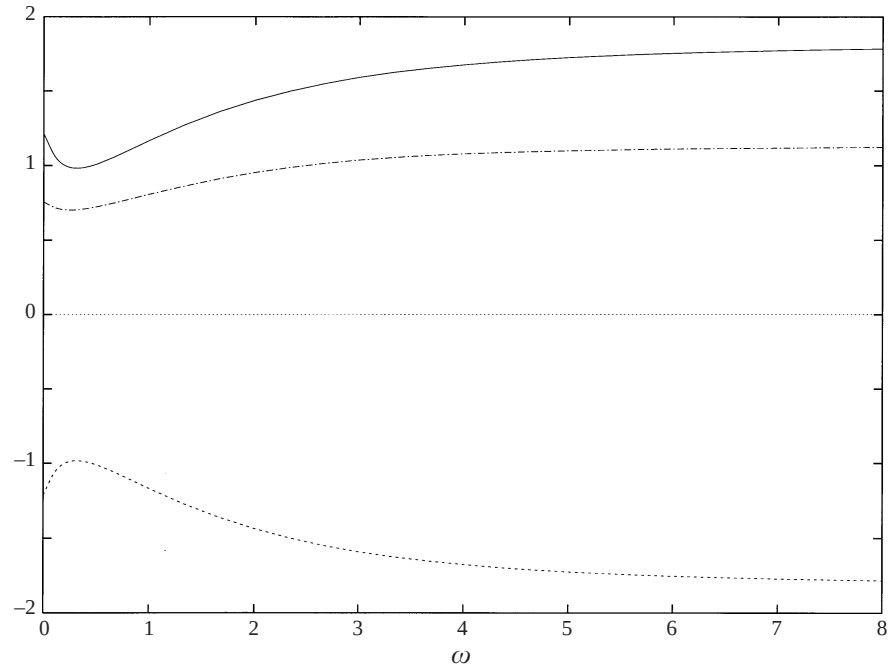

FIGURE 6. The real parts of the control impedance as functions of frequency. The distance of the source from the shear layer is 1, the sensor positions are at $z_{se} = 0.3 + 0\,\mathrm{i}$ (full), $z_{se} = -0.3$ (dashed), and at $z_{se} = 0.6$ (dot-dashed). The mean velocity U has been put to 1.

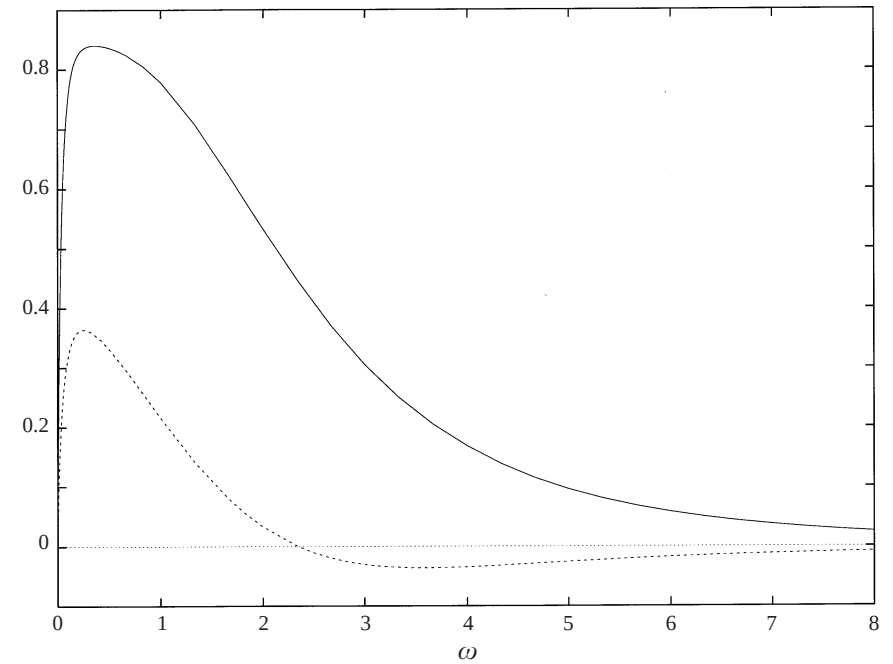

FIGURE 7. The imaginary parts of the control impedance as functions of frequency. The distance of the source from the shear layer is 1, the sensor positions are at $z_{se} = 0.3$ (full) and at $z_{se} = 0.6$ (dashed). The mean velocity U has been put to 1.

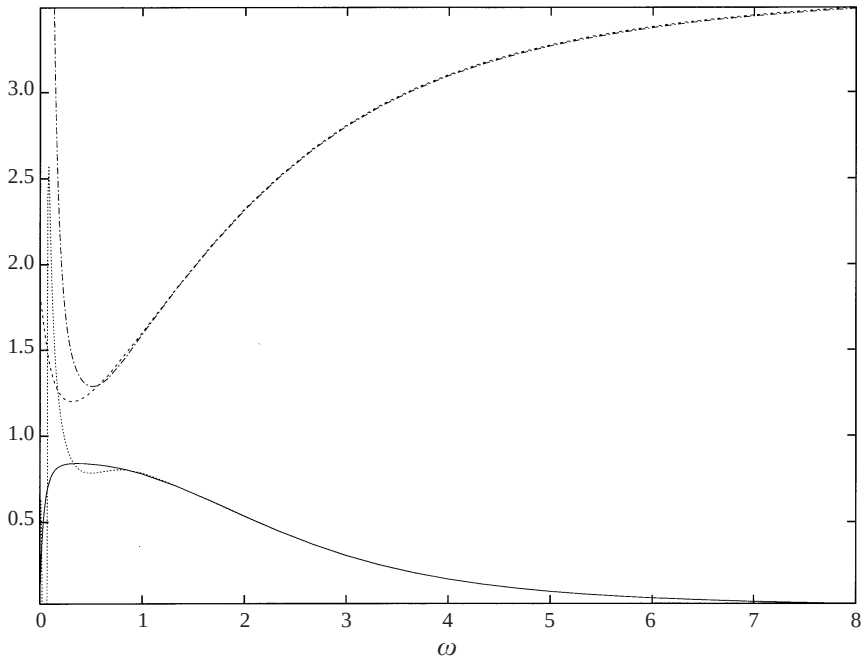

FIGURE 8. Comparison between the real (dashed) and imaginary (full) parts of the non-causal impedance of figure 6 at $z_{se} = 0.3$ and the real (dot-dashed) and imaginary (dotted) parts of a causal one which was obtained from the control of a supposed point source at $z = -5 + \mathrm{i}$ such that the potential vanishes at $z = 5$.

one. The causal impedance was obtained by shifting the generation and detection position from $-\infty$ and $+\infty$ to finite values ∓ 5. We therefore require that the actuator source is determined such that the potential of a source solution with source at $z = -5 + \mathrm{i}$ vanishes at $z = 5$ with a sensor position at $z_{se} = 0.3$. Notice that differences occur only for small frequencies. This should not be too surprising. Differences are to be expected for those frequencies where the wavelength becomes comparable with the distance to the Kelvin–Helmholtz wave generating source, i.e. 5 in figure 8. Further light is shed on the difference if one considers the Fourier tranform of the impedance from ω-space to t-space, namely the transfer function. The non-causal transfer function contains precursors, which are lacking in the causal one. Therefore the time integral over the square of the difference of the transfer functions is never smaller than that integral taken over the precursor. Then Parseval's theorem shows that the frequency integral over the modulus squared of the difference of the impedances also remains finite. Figure 8 shows that these differences can be shifted to small frequencies.

We have designed the impedance for the control of incident Kelvin–Helmholtz waves. To study its effectivity for other perturbations, the motion of the controlled shear layer with a point source has been determined. As the flow of a source in its downstream region is dominated by the Kelvin–Helmholtz wave, one expects that Kelvin–Helmholtz waves from upstream sources could be suppressed, while a source situated far downstream of the positions of the sensor and of the source could probably not be controlled. The flow field of a perturbation in the upstream region is not determined by the rapidly decaying Kelvin–Helmholtz wave, but by the slower decay of the source. The control system would therefore greatly overestimate the strength of a source situated downstream. Figure 9 shows that this is actually true.

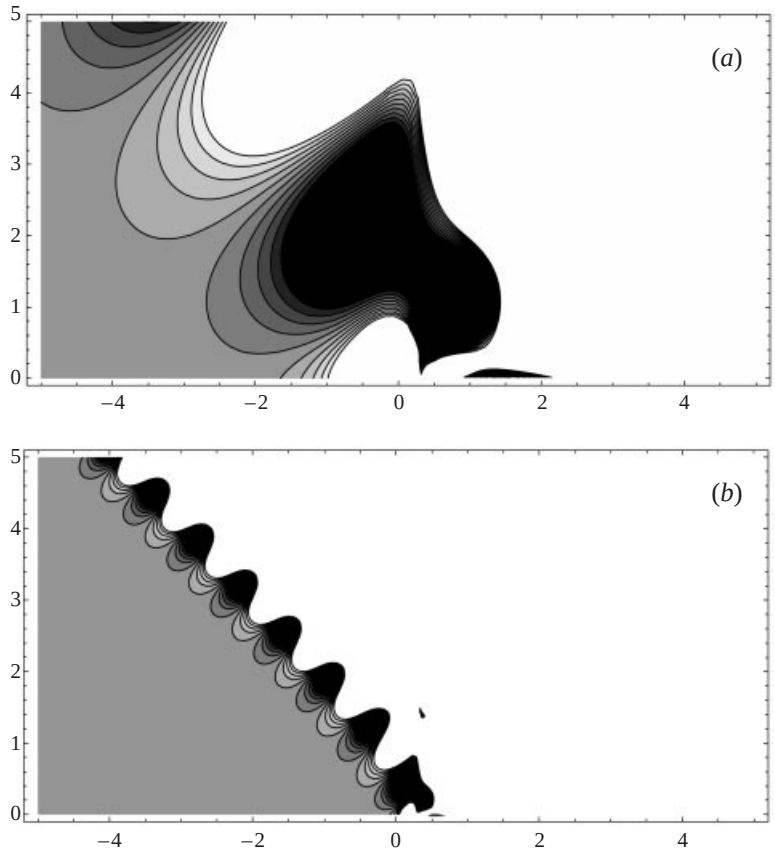

FIGURE 9. Control of point sources. Point sources positioned in the shaded part of the upper half-plane can be controlled effectively; sources $\omega = 1$ (*a*) and $\omega = 5$ (*b*). The control system sensor is at $z_{se} = 0.3 + 0\mathrm{i}$ and the actuator at $z = -\mathrm{i}$. The shading levels show the amplitude ratios of the incident and the counteracting Kelvin–Helmholtz wave. There is a balance between them for upstream sources of the initial instability, which is therefore cancelled by the control action.

There the ratio of the amplitudes of the Kelvin–Helmholtz waves of the source and of the control source are shown. Light regions indicate a dominance of the Kelvin–Helmholtz wave from the source while the Kelvin–Helmholtz wave from the control source dominates if the source is located in a dark region. Both amplitudes differ by less than 10% in regions which are not black or white. The far upstream region is gray. This indicates that a source situated there would effectively be cancelled. Only the region $y > 0$ is shown, i.e. the control of perturbations in the half-space with mean flow. The same reduction of the Kelvin–Helmholtz waves occurs for sources in the no-flow region. Figure 9(*a*) refers to $\omega = 1$ and 9(*b*) to $\omega = 5$. One observes the $\pm 45^\circ$ sector which is so characteristic for Kelvin–Helmholtz instabilities. The waviness illustrates the complicated behaviour which analytic functions show at the boundaries between regions of different asymptotic laws.

5. Conclusion

A study of the influence of a source on a shear layer has shown that the instability of a vortex sheet can be suppressed if a linear relation between the source and the velocity at an arbitrary position is assumed. It is required that the constant of

proportionality, the impedance, depends suitably on the frequency, i.e. the source strength is some functional of the velocity history at the sensor position. Then the source generates Kelvin–Helmholtz waves which are in antiphase to incident Kelvin–Helmholtz waves. This impedance turns out to be non-causal. We show that it can be approximated for most frequencies by causal ones. The control mechanism works effectively only for these frequencies. For the remaining frequencies incident Kelvin–Helmholtz waves are not completely annihilated, and they may even be amplified. A study of an initial value problem shows that a δ-function disturbance is suppressed effectively by this control in marked contrast to an uncontrolled shear layer where one meets a finite time singularity.

Most of this research was done while W. M. was the quatercentenary visiting research fellow at Emmanuel College, Cambridge.

REFERENCES

Abramowitz, M. & Stegun, I. A. 1965 *Handbook of Mathematical Functions*. Dover.

Arbey, H. & Ffowcs Williams, J. E. 1984 Active cancellation of pure tones in an excited jet. *J. Fluid Mech.* **149**, 445–454.

Bechert, D. W. & Michel, U. 1975 The control of a thin free shear layer with and without a semi-infinite plate by a pulsating flow field. *Acustica* **33**, 287–307.

Callier, F. M. & Desoer, C. A. 1991 *Linear System Theory*. Springer.

Crighton, D. G. 1985 The Kutta condition in unsteady flow. *Ann. Rev. Fluid Mech.* **17**, 411–445.

Ffowcs Williams, J. E. 1982 Sound sources in aerodynamics – fact and fiction. *AIAA J.* **20**, 307–315.

Fiedler, H. E. 1998 Control of free turbulent shear flow. In *Flow Control* (ed. M. Gad-el-Hak, A. Pollard & J.-P. Bonnet), pp. 335–429. Springer.

Jones, D. S. & Morgan, J. D. 1972 The instability of a vortex sheet on a subsonic stream under acoustic radiation. *Proc. Camb. Phil. Soc.* **72**, 465–488.

Landau, L. D. & Lifschitz, E. M. 1966 *Lehrbuch der theoretischen Physik. Bd. V. Statistische Physik*, p. 125. Akademie.

Moin, P. & Bewley, T. 1994 Feedback control of turbulence. *Appl. Mech. Rev.* **47**, S3–S13.

Möhring, W. 1975 On flows with vortex sheets and solid plates. *J. Sound Vib.* **38**, 403–412.

Ronneberger, D. & Ackermann, V. 1979 Sound from stability waves in jets. *J. Sound Vib.* **62**, 121–129.